ISBN: 978-3-95450-208-0 doi:10.18429/JACoW-IPAC2019-MOPGW094

FIRST MACHINE DEVELOPMENT RESULTS WITH HL-LHC CRAB CAVITIES IN THE SPS

L.R. Carver, C. Welsch, The University of Liverpool, Liverpool L69 7ZE, UK
A. Alekou, R. Appleby, The University of Manchester, Manchester M13 9PL, UK
G. Burt, J. Mitchell, The University of Lancaster, Lancaster LA1 4YW, UK
F. Antoniou, H. Bartosik, T. Böhl, R. Calaga, M. Carla',
T. Levens, G. Papotti, CERN, CH-1211 Geneva, Switzerland

ABSTRACT

Crab cavities are a critical component within the High Luminosity upgrade project for the Large Hadron Collider (HL-LHC). It is foreseen to use crab cavities in order to compensate the geometric luminosity reduction factor (reduction of the luminous region at the Interaction Point [IP]) due to the beam crossing angle (required for minimizing the impact of the long range beam-beam effects on the single particle beam dynamics) and increase the number of collisions per bunch crossing. In 2018 the first beam tests of crab cavities with protons were performed in the Super Proton Synchrotron (SPS) at CERN. Two vertical superconducting cavities of the Double Quarter Wave (DQW) type were fabricated and installed in the SPS to verify some key components of the cavity design and operation. This paper will present some of the first results relating to the proton beam dynamics in the presence of crab cavities.

INTRODUCTION

At present the colliding bunches in the Large Hadron Collider (LHC) do collide with a small crossing angle. This is to minimise the long range beam-beam effects. The crossing angle implies a luminosity decrease by reducing the overlapping parts of the two bunches. The High Luminosity - LHC (HL-LHC) upgrade project will enhance the performance of the LHC in a number of ways, one of which is to use a crab cavity (CC) on either side of interaction point (IP) 1 and 5 [1, 2].

CCs can be used to provide a rotational kick (positive for the head of the bunch and negative for the tail - or vice versa) to restore the luminosity reduction introduced by the crossing angle. In the local CC scheme, the bunches will still follow an angle through the insertion region (IR) but will collide at the IP head-on. CCs have been used in the past with leptons at KEK [3], but they have never been used with protons. There are many questions relating to the performance of CCs with proton beams. As part of the HL-LHC program, two superconducting CCs were fabricated and installed at the SPS to facilitate testing of both the RF design of the cavities and to provide experimental verification of some important beam dynamics principles with protons.

Initially the SPS operation setup for the CC tests will be described, then the different crabbing diagnostics will be introduced and briefly compared. Finally, some of the initial results of the CC test program will be shown.

OPERATIONAL CONSIDERATIONS

Information on the RF design of the cavities can be found in Ref. [4]. The two superconducting CCs operate at 400 MHz [4] and are installed within the same cryomodule (CM). The CM was installed in Point 6 of the SPS on a moveable table. The CCs can therefore be moved in and out of the beam path as needed without breaking the beam vacuum.

The SPS is a cycling machine with typical cycle times ranging from 1 second to approximately 40 seconds. In order to perform the desired CC manipulations within the existing framework used to control the SPS, two longer-than-average cycles were created specifically for the CC measurements. The first cycle can take multiple Proton Synchrotron (PS) injections and has a flat-bottom plateau of 19.2 s at the injection energy of 26 GeV, and the second can take one PS injection and then ramps from 26 GeV to 270 GeV where it has a flat-top plateau of 26.6 s.

At the end of the injection period, the SPS main RF (at 200 MHz) is re-phased to become synchronous with the CC RF signal (at 400 MHz). This to ensure that the phasing between the beam and the CC is constant. Therefore the beam will experience the same CC phase each turn.

During the experimental campaign, a range of beam and machine parameters were used and can be found in Table 1.

Table 1: The Range of Machine and Beam Parameters Used During the Experimental Campaign

Parameter	Value	Unit
Energy	26, 270	GeV
Tune Q_x, Q_y	26.13, 26.18	...
Chromaticity Q'_x, Q'_y	2-5, 2-5	...
Number of Bunches M	1-72	...
Bunch intensity N_b	0.2-1.2	$10^{11}p$
Bunch norm. emit. ε_x, ε_y	1.5-2.5, 1.5-2.5	μm
Bunch length 26 GeV $4\sigma_t$	2.75-3	ns
Bunch length 270 GeV $4\sigma_t$	1.4-1.8	ns
CC Peak Voltage V_1, V_2	1, 1	MV

CRABBING DIAGNOSTICS

There are several different ways to measure the effect of the crab cavity on the proton beam. This can be with a direct measurement of the intra-bunch offset or by recording closed orbit shifts. Each method relies on the principle of making a measurement of the bunch (or bunch slice) offset at one

ISBN: 978-3-95450-208-0 doi:10.18429/JACoW-IPAC2019-MOPGW094

location and calculating the kick required at the crab cavity location to reconstruct the observation. The general formula for calculating the orbit shift from a kick is given by [5]

$$u_i = \frac{\sqrt{\beta_i}}{2\sin(\pi Q)} \sum_{j=i+1}^{i+n} \theta_j \sqrt{\beta_j} \cos(\pi Q - |\psi_i - \psi_j|), \quad (1)$$

where i is the observation location, j is the location of the kick, β is the beta-function, Q is the tune, ψ is the phase (in tune units) and θ is the kick. In the case of a crab cavity, the kick can be expressed as $\theta_j = -\frac{qV(t)}{W}$, where q is the particle charge, W is the beam energy and $V(t)$ is the time dependant voltage a particle experiences while traversing the CC. The crab cavities are next to each other, so the difference in beta-function is small and the betatron phase advances by a small amount between them. Therefore both cavities can be approximately combined into one kick which has a voltage that is given by

$$V(t) = V_1 \sin(\omega t + \phi_1) + V_2 \sin(\omega t + \phi_2) \quad (2)$$

where the 1 and 2 subscripts refer to CC1 and CC2 respectively, V is the cavity voltage, $\omega = 2\pi f$ where f is the cavity frequency and ϕ is the phase of the cavity. Therefore in order to recalculate the kick at the CCs from an offset measurement at an observation point, one only needs information of the beta-functions and the vertical betatron phases at both the CCs and the location of the diagnostic device.

Headtail Monitor

The headtail monitor is a stripline pickup with a fast scope that is capable of rapidly processing the analogue signals to provide a digitized output of the intra-bunch offset. The monitor installed in the SPS is very similar to the one installed in the LHC [6]. This offset was calibrated to the orbit Beam Position Monitors (BPMs - introduced in the next section) at the end of 2017. The headtail monitor was the primary crabbing diagnostic device in 2018. It is triggered once per cycle and has a resolution of 100 ps (compared to bunch lengths of 2.9 ns).

MOPOS BPM

The SPS has a series of Beam Position Monitors (BPMs) installed throughout the ring for orbit measurements. The Multi Orbit Position System (MOPOS) BPMs measure the closed orbit with 80 horizontal BPMs and 113 vertical BPMs [7]. As shown in Ref. [1], a crab cavity kick will introduce a crab dispersion which will alter the closed orbit as a function of position (or displacement from synchronous particle) along the bunch. This will be able to be directly measured by the BPMs.

In order to measure the effect of the crab cavity on the orbit, two acquisitions are needed. The first measurement should be with crab cavities off to acquire the reference closed orbit. Then another acquisition can be taken with a certain CC kick. The reference closed orbit can then be removed and the cavity voltage can be calculated. A simple optimization can be performed using MAD-X where a dipolar kick is applied at the location of the CC and the strength of this kick is optimized to match the measured closed orbit with the closed orbit from MAD-X.

DOROS BPM

Also installed in the SPS are Diode Orbit & Oscillation (DOROS) BPMs [8]. These BPMs reverse the polarity of the electronics processing with a switching frequency of 1 Hz and then averages the measurements over 0.5 Hz. This averaging effect helps to reduce the noise level and provide a more accurate measurement of the closed orbit. There are 4 DOROS BPMs in the SPS, with 2 DOROS BPMs installed either side of the crab cavity CM.

The DOROS BPMs publish a value for the orbit once per second, with each measurement averaging over the previous two seconds. As described in the previous section, the crab cavities are not powered until the SPS main RF becomes phase locked with the crab cavities. For some sets of measurements, the CC RF was only switched on half way through the cycle. This means that within one cycle the closed orbit without CCs and with CCs can be obtained, allowing the orbit shift at the location of the DOROS BPM to be measured. Once the orbit shift has been measured, the kick and therefore the voltage are recalculated.

When analysing the data from the BPMs (both MOPOS and DOROS), it is important to account for any filtering that occurs during the processing of the signals. The MOPOS BPMs have a 200 MHz narrow band filter, while the DOROS BPMs have a low pass filter up to 200 MHz. The presence of a 400 MHz signal in the beam affects the output after the filtering.

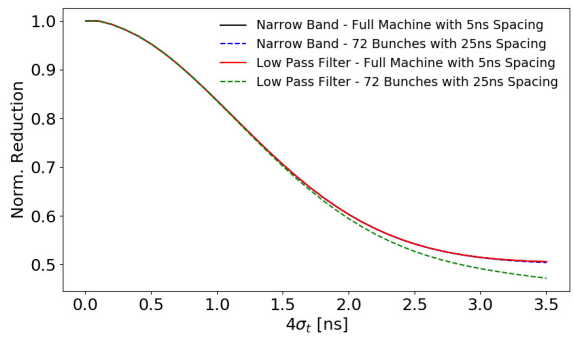

Figure 1: The normalised BPM readout as a function of bunch length for different types of filters and beam parameters. The bunch length at 26 GeV is $4\sigma_t \approx 2.9$ ns and at 270 GeV it is $4\sigma_t \approx 1.4$ ns.

Figure 1 shows the normalised BPM output versus bunch length for two different filling configurations. The first is a full machine (or beam with inifinite bunches) with 5 ns bunch spacing. i.e. every single bucket is filled. The second is a more realistic filling scheme, with 72 bunches with 25 ns

ISBN: 978-3-95450-208-0 doi:10.18429/JACoW-IPAC2019-MOPGW094

spacing but also including the rest of the machine which does not contain beam. Each cases produces slightly different signals in the frequency domain. It can be seen that the resonant filter behaves identically for realistic trains vs a continuous bunched beam. However for the low pass filter, the results are slightly different depending on the number of bunches in the 25 ns train, this behaviour approaches the narrow band filter as the number of bunches increases.

FIRST RESULTS

Measurement of Crabbing

A phase scan was made in CC2 with a fixed voltage, while the phase and voltage of CC1 was kept constant. This allowed a comparison of the cavity voltage between all the diagnostic devices. The results of this scan can be found in Table 2. It can be seen that the power sensors that convert the forward power to cavity voltage show a slightly lower voltage than is measured from beam based diagnostic devices. This conversion requires the external quality factor of the field antenna Q_e. $Q_e = 1.6 \times 10^{10}$ is used (from simulation) but $Q_e = 1.79 \times 10^{10}$ could give good agreement with the rest of the devices.

Table 2: A Summary of the Measured Crab Cavity Voltage from the Different Diagnostic Devices in the SPS

Device Name	Voltage [MV]
Power Sensors	0.98
Headtail Monitor	1.23
MOPOS BPMs	1.39
DOROS BPM 51805	1.21
DOROS BPM 51999	1.33
DOROS BPM 61736	1.25
DOROS BPM 61751	1.25

The rest of the diagnostic devices show good agreement, with possible discrepancies arising from the sensitivity of each device.

Cavity Transparency

The CCs were placed in counter phase with 1 MV per cavity in order to see if the total crabbing kick can be cancelled. This was done manually by first placing the cavities in the maximum crabbing phase which corresponded to a maximum crabbing kick of 2 MV. Then the phases were reversed in one cavity, and the phases were fine tuned to minimize the crabbing signal. The two cases can be seen in Fig. 2.

The lowest crabbing voltage that was achievable was equivalent to a crabbing kick of 60 kV (compared to 2 MV total). With future automation of this procedure it is probable that this measurement can be reduced further.

Other Measurements

Other measurements that were made during the CC experimental program are also presented at this conference. Beam

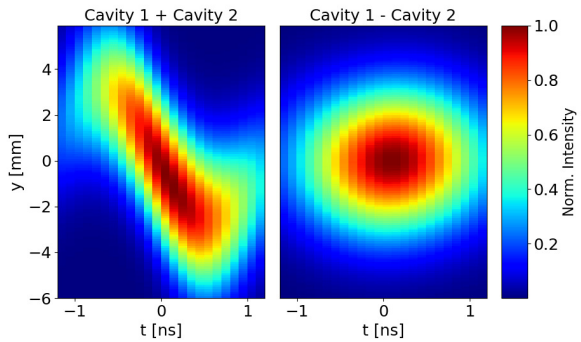

Figure 2: Headtail monitor acquisitions comparing two cases which show the CCs in phase (left) and cancelling (right).

based measurements on the skew sextupolar component of the crab cavities can be found in Ref. [9]. Results relating to the comparison of the analytical predictions [10] and measurements of the emittance growth in coast are scheduled to be published soon Ref. [11]. Some observations relating to machine protection can be found in Ref. [12].

CONCLUSIONS

The crab cavity prototype for HL-LHC has been installed in the SPS and used for the worlds first tests of crab cavities with protons. The results from these tests provide important information on the RF design of the crab cavities as well as what operational steps will be needed in the HL-LHC era. This information will be used to update and improve the design of the HL-LHC crab cavities and other lessons learnt from these tests will help plan future Crab Cavity tests in the SPS.

ACKNOWLEDGMENTS

This research is supported by the HL-LHC project and the STFC through HLLHCUK collaboration. The authors would like to thank Y. Papaphilippou, J. Resta-Lopez and A. Dexter for fruitful discussions and important contributions.

REFERENCES

[1] Y.P. Sun, R. Assmann, J. Barranco, R. Tomás, T. Weiler, F. Zimmermann, R. Calaga, A. Morita, 'Beam dynamics aspects of crab cavities in the CERN Large Hadron Collider', Phys. Rev. ST Accel. Beams 12, 101002, (2009).

[2] J. Barranco, R. De Maria, A. Grudiev, R. Tomás, R.B. Appleby, D.R. Brett, 'Long term dynamics of the high luminosity Large Hadron Collider with crab cavities', Phys. Rev. Accel. Beams 19, 101003 (2016).

[3] K. Ohmi, M. Tawada, Y. Cai, S. Kamada, K. Oide, J. Qiang, 'Luminosity limit due to the beam-beam interactions with or without crossing angle', Phys. Rev. ST Accel. Beams 7, 104401 (2004).

[4] S. Verdú-Andrés, K. Artoos, S. Belomestnykh, I. Ben-Zvi, C. Boulware, G. Burt, R. Calaga, O. Capatina, F. Carra, A. Castilla, W. Clemens, T. Grimm, N. Kuder, R. Leuxe, Z. Li,

ISBN: 978-3-95450-208-0 doi:10.18429/JACoW-IPAC2019-MOPGW094

E.A. McEwen, H. Park, T. Powers, A. Ratti, N. Shipman, J. Skaritka, Q. Wu, B.P. Xiao, J. Yancey C. Zanoni, 'Design and vertical tests of double-quarter wave cavity prototypes for the high-luminosity LHC crab cavity system', Phys. Rev. Accel. Beams 21, 082002 (2018).

[5] A.W. Chao, K.H. Mess, M. Tigner, F. Zimmermann, 'Handbook of Accelerator Physics and Engineering', Second Edition, World Scientific (2012).

[6] T.E. Levens, K. Lasocha, T. Lefevre, 'Recent Development for Instability Monitor at the LHC', Proceedings of the 5th International Beam Instrumentation Conference, Barcelona, Spain, THAL02, pp.852-855 (2016).

[7] C. Boccard, T. Bogey, J. Brazier Ltd, J. de Vries, S. Jackson, R. Jones, J.P. Papis, W. Rawnsley, K. Rybaltchenko, H. Schmickler. 'Performance of the new SPS Beam Position Orbit System (MOPOS)', Proceedings of DIPAC 1999, Chester, UK (1999).

[8] J. Olexa, O. Ondracek, Z. Brezovic, M. Gasior, 'Prototype system for phase advance measurements of LHC small beam oscillations', CERN-ATS-2013-038, CERN, Geneva, Switzerland (2013).

[9] M. Carla' *et al*, 'Beam-Based Measurement of the Skew-Sextupolar Component of the Radio Frequency Field of a HL-LHC-Type Crab-Cavity', this conference, IPAC19, Melbourne, Australia, (2019) MOPTS090.

[10] P. Baudrenghien, T. Mastoridis, 'Transverse emittance growth due to rf noise in the high-luminosity LHC crab cavities', Phys. Rev. ST Accel. Beams 18, 101001 (2015).

[11] P. Baudrenghien, T. Mastoridis, E. Yamakawa, 'Measurements of transverse emittance growth due to rf noise in the SPS', *to be published*

[12] B. Lindstrom, H. Bartosik, T. Bohl, A. Butterworth, R. Calaga, L. Carver, V. Kain, T. Levens, G. Papotti, R. Secondo, J. Uythoven, M. Valette, G. Vandoni, J. Wenninger, D. Wollmann, M. Zerlauth, 'Machine Protection Experience from Beam Tests with Crab Cavity Prototypes in the CERN SPS', this conference, IPAC19, Melbourne, Australia (2019), MOPMP036.